2013

Investigation of the Physical Phenomena Associated with Rain Impacts on Supersonic and Hypersonic Flight Vehicles

Bruce Moylan
U.S. Army Aviation and Missile Research, bruce.moylan@us.army.mil

Brian Landrum
University of Alabama - Huntsville

Gerald Russell
U.S. Army Aviation and Missile Research

Available online at www.sciencedirect.com

SciVerse ScienceDirect

Procedia Engineering 58 (2013) 223 – 231

Procedia Engineering

www.elsevier.com/locate/procedia

The 12th Hypervelocity Impact Symposium

Investigation of the Physical Phenomena Associated with Rain Impacts on Supersonic and Hypersonic Flight Vehicles

Dr. Bruce Moylan[a]*, Dr. Brian Landrum[b], Dr. Gerald Russell[a]

[a] U.S. Army Aviation and Missile Research, Development, Engineering Center
5400 Fowler Road, Redstone Arsenal, AL 35898, USA
[b] University of Alabama in Huntsville
301 Sparkman Drive, Huntsville, AL 35899, USA

Abstract

The U.S. Army AMRDEC has been performing research focusing on both analytical modeling and obtaining validation data through experimentation. The focus of this research is to understand both the impact event, and the associated material damage mechanisms. A key aspect of weather encounter modeling is that the local vehicle flow field environment alters the impact boundary conditions with time. Therefore, an analytical model must be able to include not only the vehicle flow field, but also the time accurate embedded flow field surrounding the droplets as they alter shape prior to impact. The impact event is highly dependent on the actual droplet shape at impact, and therefore extensive modeling and testing was required to obtain data suitable for code validation. The empirical testing effort consisted of single droplet impacts, high-speed rocket sled testing, and testing in a ballistics range. The data presented focuses on the data collected at the ballistics range for Mach numbers ranging from 2 to 7 for various shapes. The core analytical effort was developed by extensive modifications of the Smoothed Particle Hydrodynamics C-Code (SPHC) from Stellingwerf Consulting, augmented with an improved water equation of state that included the supercooled regime to augment the fidelity of the impact physics for rain drops at high altitudes. The analytical model demonstrates that the temporal distortion of water in a post-shock environment and the impact events for various projectiles can be captured with reasonable accuracy. The next step is to obtain data within the shock layers of relevant vehicle shapes in order to obtain the detailed demise and coupled flow field physics in order to validate the model in a realistic environment. The data presented reveals the droplet shape change and demise characteristics inside the shock structures for missile domes and sphere-cone designs, along with the complex embedded shock structure and impact physics associated with these events. This data forms a subset of empirical data that can be used for the fully-coupled full-scale impact events on flight vehicles.

Selection and peer-review under responsibility of the Hypervelocity Impact Society

Keywords: Droplet demise, high-speed weather enconter, smoothed particle hydrodynamic modeling, ballistic range testing

Nomenclature

D	Diameter
V	Velocity
We	Weber Number
Greek symbols	
θ	Angle between the vehicle velocity vector and the post-shock air velocity vector
σ	Surface tension

* Corresponding author. Tel.: + 1-256-313-2236;
E-mail address: bruce.moylan@us.army.mil.

1877-7058 © 2013 The Authors. Published by Elsevier Ltd.
Selection and peer-review under responsibility of the Hypervelocity Impact Society
doi:10.1016/j.proeng.2013.05.026

ρ	density

1. Introduction

It is well known that high-speed flight through natural weather poses a significant design challenge to the vehicle designer. The severity of the environment increases exponentially with velocity and the damage associated with high-speed weather encounter can be quite severe, and in some cases, can become a limiting factor [1]. Adverse weather environments that may be encountered by flight vehicles range from hydrometeors such as rain, sleet, hail, graupel, snow, and ice, to solid airborne particulates such as sand, dust, and volcanic ash. The importance of each of these natural elements as it relates to vehicle damage is a strong function of the system's flight velocity, geometry, and required precision or damage tolerance.

As rain encounter forms the primary environment for flight systems that have any portion of their flight envelope below an altitude of 4 km, being able to simulate the impact event on a laboratory scale has broad applicability for many flight systems. Rain is unique in that it strongly interacts with the vehicle induced flow field thereby creating highly complex impact conditions. For most other forms of adverse weather, the particles may be deflected in the post-shock flow, but they do not significantly change shape or lose mass. Raindrops however can be significantly deformed in the post-shock flow field, making it difficult to estimate the impact damage potential. Understanding raindrop demise and shape change caused by the coupled interaction of the droplet with the high-speed vehicle flow field is therefore a necessary precursor to predicting the expected system response for any real-world weather condition.

The importance of this research is that the impacting force, and subsequent vehicle damage, is a function of the drop state at the moment of impact. Because the droplets are distorted in the post-shock flow field environment, suitable ground tests are difficult to perform unless one tests a full-scale vehicle at flight-like conditions. As this is exceedingly difficult and costly, subscale component tests are commonly performed, but unless the correct impact conditions are precisely known, the damage and the subsequent damage models developed will not match the actual flight environment. Such uncertainty will produce misleading performance estimates and result in an unknown system capability. The challenge therefore is to be able to understand the droplet distortion for a full-scale vehicle, and to recreate that environment in the laboratory or other ground test facilities.

However, the challenge is that vehicle induced drop demise has both a temporally varying droplet imbedded in a temporally varying flow. The complexity of this fully-coupled environment has typically been reduced in order to make the testing and response model development effort more tractable, but the appropriateness of these assumptions have largely been unverified. Employing these assumptions, shock tubes have been historically utilized with a steady post-shock flow. The objective of this work is to determine if the historical assumptions are valid for common vehicle geometries.

2. Droplet Distortion in a Shock Tube Environment

There have been numerous droplet demise studies in shock tubes spanning several decades [2, 3, 4, 5]. These studies provide sufficient data to obtain a validation set for almost any numerical model effort. Except for the work of Theofanous [6, 7] however, the data from all previous efforts consisted of mainly shadowgraphs, derived drag, and lateral expansion estimates, and as such could only be used in a qualitative fashion. The work of Theofanous however utilized an innovative laser fluorescence technique and was able to capture qualitative details of the temporal droplet shape. In contrast to the significant volume of shock tube data, there have been few analytical efforts attempting to model the problem [8] and none utilizing the data of Theofanous. This section provides a brief overview of the numerical validation effort with the data of Theofanous. Additional details associated with the development of this numerical model can be found in reference [9]. Once the numerical model has been validated with the steady flow environment of shock tubes and tunnels, the model can then be used as a tool to investigate the more complex vehicle flow field. Figure 1 shows the time sequence of a droplet demise event in a shock tunnel flow.

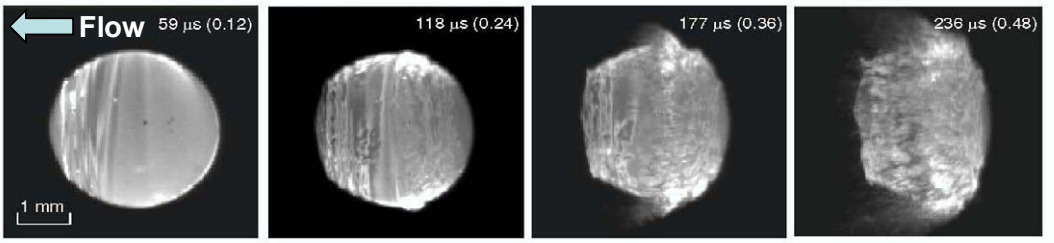

Fig. 1. Demise photographs the droplet distortion process in a Weber = 5400 Flow [2]

The empirical data has sufficient clarity as to enable the extraction of key dimensional features as a function of time. The quantitative parameters derived from these experiments are shown in Fig. 2. There were seven key features extracted from the data at two different times. The comparison of the empirical data to the numerical model is shown in Table 1.

The empirical data has sufficient clarity as to enable the extraction of key dimensional features as a function of time. The quantitative parameters derived from these experiments are shown in Fig. 2. There were seven key features extracted from the data at two different times. The comparison of the empirical data to the numerical model is shown in Table 1. The average of each of the seven measurements for each time frame was within 8% of the data. The maximum discrepancy for any measurement was 31% which corresponded to the axial distance from the stagnation point of the drop to the location of the stripping crest wave. However, the critical dimensions for estimating surface impact damage are the frontal radius of curvature (G), the overall depth (C), and width of the droplet (E). Considering these dimensions, the numerical model was able to predict the test data to within 14%. This comparison provides the needed model validation in order to move on to the next phase of the problem and address the vehicle flow field.

Table 1. Numerical and Empirical Feature Correlation

Location	177 μsec (mm)			236 μsec (mm)		
	Data	SPHC	Diff	Data	SPHC	Diff
A	0.63	0.68	1.08	-	0.66	-
B	1.28	1.57	1.23	1.21	1.59	1.31
C	2.64	2.71	1.03	2.43	2.48	1.02
D	3.14	3.44	1.10	3.00	3.60	1.20
E	3.9	4.18	1.07	4.23	4.38	1.04
F	2.21	2.43	1.10	2.47	2.53	1.02
G	2.29	2.17	0.95	2.72	2.33	0.86
		Avg	1.08		Avg	1.08

3. Understanding the Vehicle Induced Flow Environment

In order to extend this work to time varying flow fields that are strongly coupled to the shape of the drop at any given instant, the differences between a vehicle induced flow, and that of shock tubes needs to be understood. The droplet-vehicle environment is shown schematically in Fig. 3. Here the post shock velocity (V_2) is equivalent to the shock tube environment only immediately after the shock on the vehicle centerline if the vehicle is at zero degrees angle-of-attack (AoA). At no other place in a vehicle shock environment is the shock tube environment an exact solution. Velocity (V_D) is the actual time varying velocity that the droplet experiences. Computational fluid dynamic calculations with the proper coordinate transformation, shows that the droplet velocity increases as the droplet moves closer to the vehicle. In order to highlight these differences, the Weber number is plotted for various vehicle streamlines (Fig. 4).

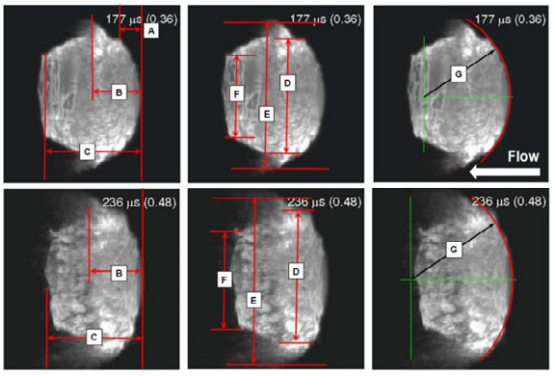

Figure 2. Feature extraction data @ 177 and 236 μsec [2]

Fig. 2. Feature extraction data at 177 and 236 msec [2].

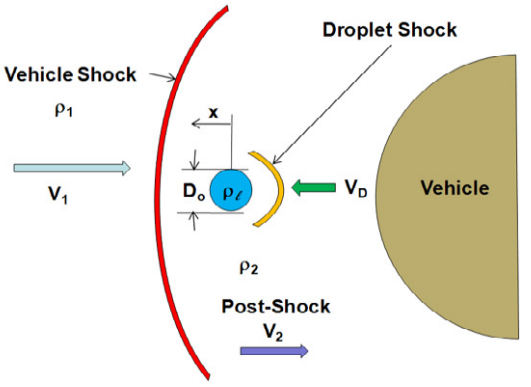

Fig. 3. Droplet demise schematic with variable references [9].

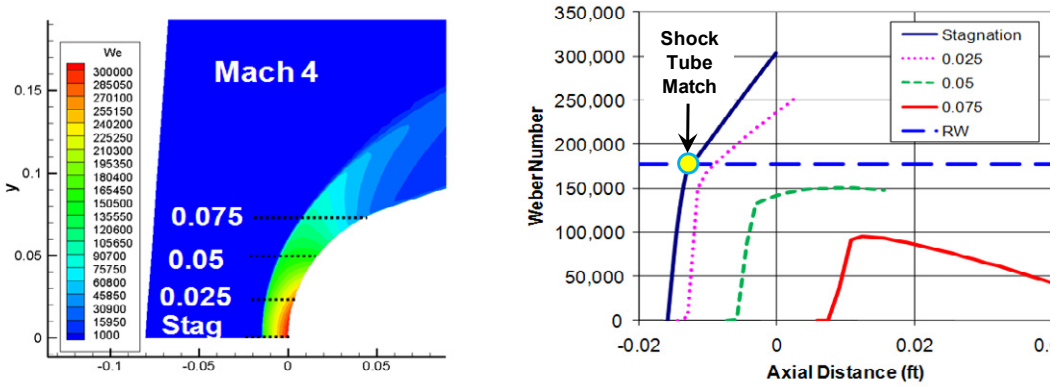

Fig. 4. Stagnation region Weber number contours.

$$We = \frac{\rho V^2 D}{\sigma} \tag{1}$$

The Weber number is the ratio of the inertial forces to the droplet surface tension and is one of the critical parameters governing droplet shape change and demise. Figure 4 shows four different streamlines along with the shock tube environment (RW) for identical freestream flow conditions. As stated previously, for a vehicle at zero degrees AoA, the shock tube environment identically matches the vehicle induced environment immediately behind the shock which can be seen at the intersection of the stagnation streamline with the shock tube (RW) curve. However, as the droplet moves deeper into the vehicle induced flow, the Weber numbers increase and at impact are approximately 75% greater than the shock tube condition for identical initial conditions. As the droplet entrance location is radially moved away from the centerline, both the magnitude and the temporal Weber number variation changes. This example serves to highlight that the droplet environment for actual flight vehicles is a function of the vehicle geometry, velocity, altitude, attitude, and shock entry location. As shock tubes create a constant Weber number condition, there is no data in the literature for droplet demise in a time varying flow, and consequently no data for numerical model validation. In order to address this deficit, a program was established to look at droplet demise and impact in vehicle induced flow conditions.

4. Droplet Impact in a Vehicle Induced Flowfield

In order to begin to obtain the required empirical data for numerical code development, two testing efforts were executed. The first effort was coordinated with NASA Marshall Space Flight Center (MSFC) using their existing test facilities with novel upgrades. This effort utilized subscale vehicle stimulants in order to produce the desired flow conditions. An example of this pathfinder effort is shown in Fig. 5. For these tests, the projectile diameter was 19-mm, the impact droplet was 4-mm in diameter, and the impact velocity was Mach 3 (1020 m/s). The photograph reveals complex physical phenomenon that occurs immediately after a droplet impact. This photograph highlights two key features of a droplet's impact on a vehicle's surface. First, the drop does not vaporize at these conditions but instead fragments into a fine mist. Secondly, this mist possesses a velocity that is greater than the impacting vehicle which distorts the vehicle induced bow shock. The vehicle bow shock is further altered by the addition of the droplet mass within the post shock flow. The addition of the droplet mass increases the density behind the shock and the vehicle bow shock equilibrates to a new location and shape. This was shown to be numerically predicted for full-scale rocket sled test hardware simulations [10]. The droplet impact also disrupts the vehicle's aerodynamic boundary layer producing an un-quantified effect on the aerodynamic heating, boundary layer state, and downstream turbulence level. Subsequent droplet impacts will amplify these effects to further alter all aspects of the vehicle flow field far downstream of the actual droplet impact point. While these effects are outside the scope of this work, it is an area of future research. While this effort aided in highlighting some of the unique physics of a droplet impact on a flight vehicle, more insight was required to develop the vehicle impact boundary conditions.

5. Ballistic Range Droplet Demise

To obtain data on the droplet demise event for realistic flight vehicles, the ballistics range at the University of Alabama in Huntsville (UAH) was utilized. This ballistics range is capable of launching projectiles of 15.2 cm in diameter and 9 kg in weight to supersonic velocities. A picture of the facility is shown in Fig. 6. The facility required an upgrade of a rain dripper system to be installed in order to provide the required droplet environment. A dripper system was designed following the work of Dabora [11], fabricated, and installed in the range to produce eleven separate streams of drops for the tests. The droplet size could be varied by utilizing different tube sizes and by varying the vibration frequency. The pre-installed dripper system is shown in Fig. 7, and a schematic of the apparatus set-up in shown in Fig. 8. While no attempt was made to simulate an actual natural rain event, but to investigate the droplet flow field interaction of the rain encounter event, the droplet densities tested are within a reasonable bound of natural events.

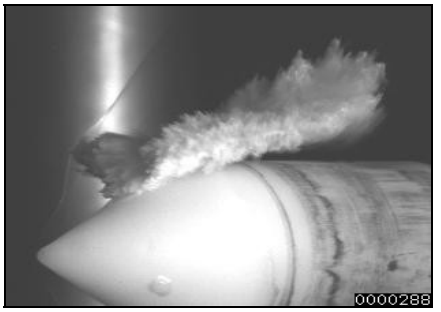

Fig. 5. Projectile impact of a 4-mm water drop. (Courtesy of NASA MSFC)

Fig. 6. UAH Ballistics Range

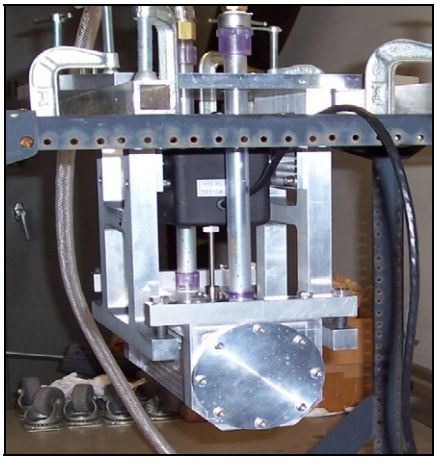

Fig. 7. Rain field dispensing dripper system.

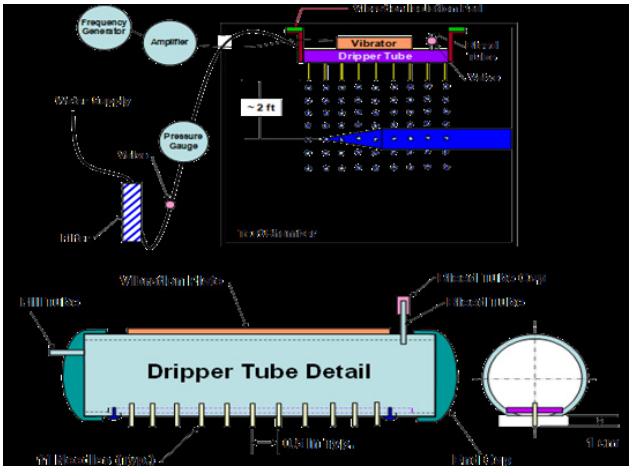

Fig. 8. Rain field dripper system schematic.

There were three basic “vehicle” shapes tested for this effort. The first was a pathfinder shape that consisted of a sphere cylinder with a base flare for stability. The diameter of the cylinder was 9.06-mm. The scale of this projectile was on the order of the droplet size which had a diameter of 6-mm. The projectile impacted a droplet on the centerline and a frame of the data is shown in Fig. 9 along with a numerical simulation of the impact event. As with the previous work, the impacting drop shatters into a fine mist and the impact event causes a impact shock wave that radically alters the pre-impact vehicle bow shock. The effect of the impact event is not localized, but significantly alters the downstream vehicle flow environment. The numerical impact predictions were developed using the Smoothed Particle Hydrodynamics C (SPHC) code from Stellingwerf consulting [12]. The SPHC code is a Lagrangian solver which utilizes a “mesh-less” technique that

models particles. As a consequence, the SPHC code is capable of modeling extreme deformations. Each "particle" contains a fixed mass at a given location and is defined by a smoothing function. The smoothing function defines a particles specific region of influence. The local mass density is a summation of all of the particles multiplied by their smoothing function at that point. The particle velocity is determined by the conservation of momentum. The particle internal specific energy is determined by the conservation of energy equation, and the flow field turbulence is modeled using a turbulent viscosity similar to many CFD solvers. In order to model this experiment, the code was upgraded with a new water equation of state, and new boundary condition options.

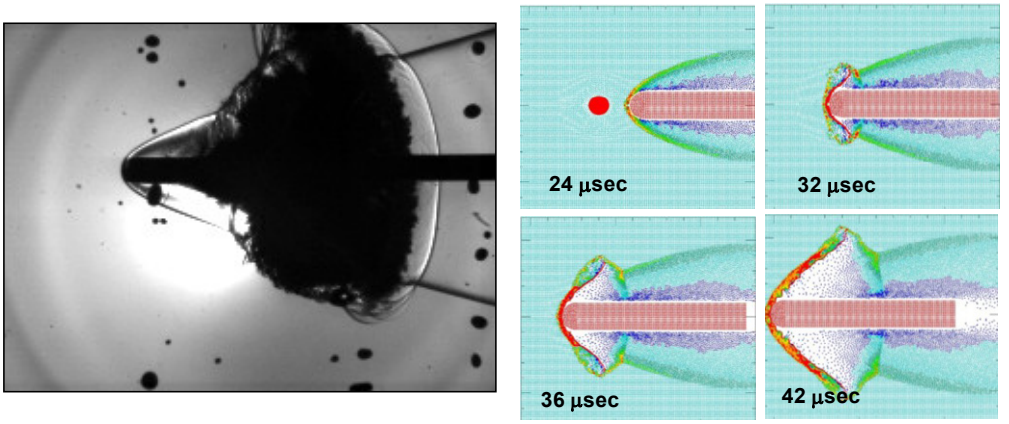

Fig. 9. Mach 4.6 Impact of a Water Drop (contour plots are in density units)

The numerical results indicate that an impact shock will form causing a significant disruption of the vehicle bow shock. While the model properly captures the radial detonation wave expansion, the data indicates that the vehicle shock will reform after the event. The model does not capture the reformation process because the numerical surface tension modeled is too great to sufficiently capturing the droplet shattering event. The numerical surface tension treatment must be upgraded in order to properly account for the droplet shattering phenomenon. However, the numerical approach is capable of capturing sufficient elements of the physics in order to be used as a guide for further testing and to highlight necessary numerical upgrades.

At this point in the program, the post-impact environment has been investigated, but the actual demise and droplet shape change has not been captured. In order to accomplish this, the projectile scaled needed to be increased so that there were sufficient time and space for the high-speed cameras to capture the details of the event. For this, the scales of the projectiles were increased to 15.2 cm diameters.

The initial projectile shape is shown in Fig. 10 and had a frontal cone angle of 12 degrees; it was over 66 cm in length, and had a nosetip radius of 0.63 cm. Due to the free flight nature of the projectile, and the need for a small camera field-of-view (FOV), each test captured different views of the impact environment which helped highlight additional details of the impact events. The first test captured a near normal impact of the droplet streams. The droplets in the FOV are 2-mm in diameter. As the previous tests were of projectiles whose physical dimensions were of comparable size to the impacting drops, this data will highlight the role of scale on the impact event. Fig. 11 shows three frames captured of the impact event. It can be seen that the shock stand-off distance for this test was insufficient to capture the droplet flow field

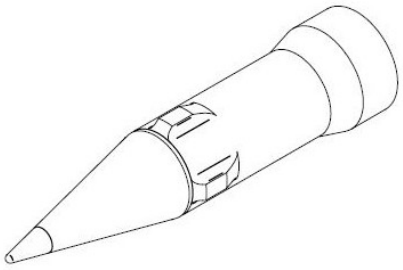

Fig. 10. Vehicle Impact Projectile

interaction in the nosetip region, but it did highlight the intensity of the impact event on the vehicle flow field. While the vehicle to droplet scale significantly increased, the effect on the flow field has not diminished, and the implication of multiple droplet impacts is clear. A vehicle traversing a rain field will experience a significant disruption of its flow field with a resulting impact on the state of the boundary layer, aerothermal heating, and possibly aerodynamics. These effects will persist well beyond the localized impact point.

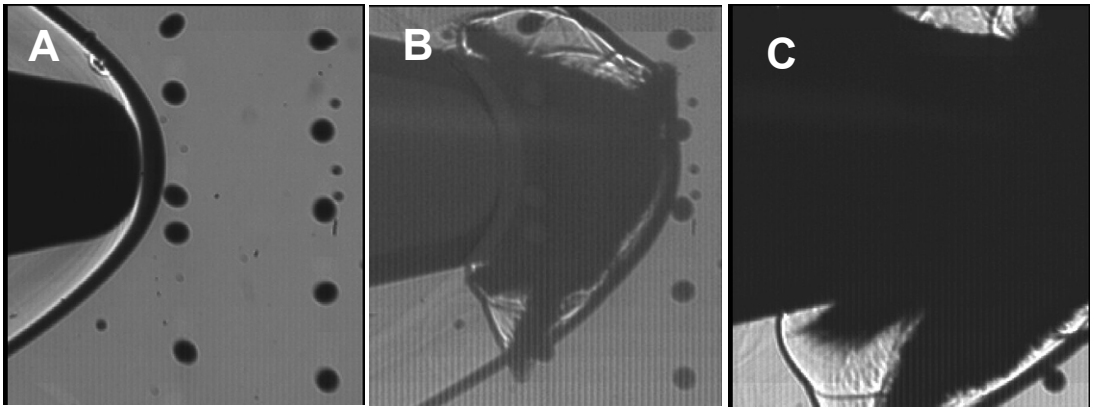

Fig. 11: Sphere cone projectile, 1026 m/s impact

In order to capture more of the post-shock vehicle flow field, a second test was conducted with an increased camera FOV, and the center of the FOV elevated to avoid the nosetip region. The results of this test are shown in Fig. 12. For this test, the droplet sizes ranged from 1 to 2-mm in diameter. The times noted in the figure are the time from the highlighted droplets entrance into the post vehicle shock flow. The two colored circles (red, blue) are focused on the time evolution of the demise event for a cluster or drops. It can be seen that as the droplets demise, the effective diameters expand. This is due to both lateral droplet dilation with time as well as an apparent size increase due to the mist being stripped from the drop's polar equator. The figure also shows the spherical shock waves caused by previous drop impacts and the droplet mist emanating from the projectile's surface. These droplet impact shock waves superimpose with the shock waves of nearby droplet impacts producing a complex flow environment that cannot be captured with conventional computational fluid dynamics codes. This data also shows that the relative droplet velocity vector can be approximated to be normal to the

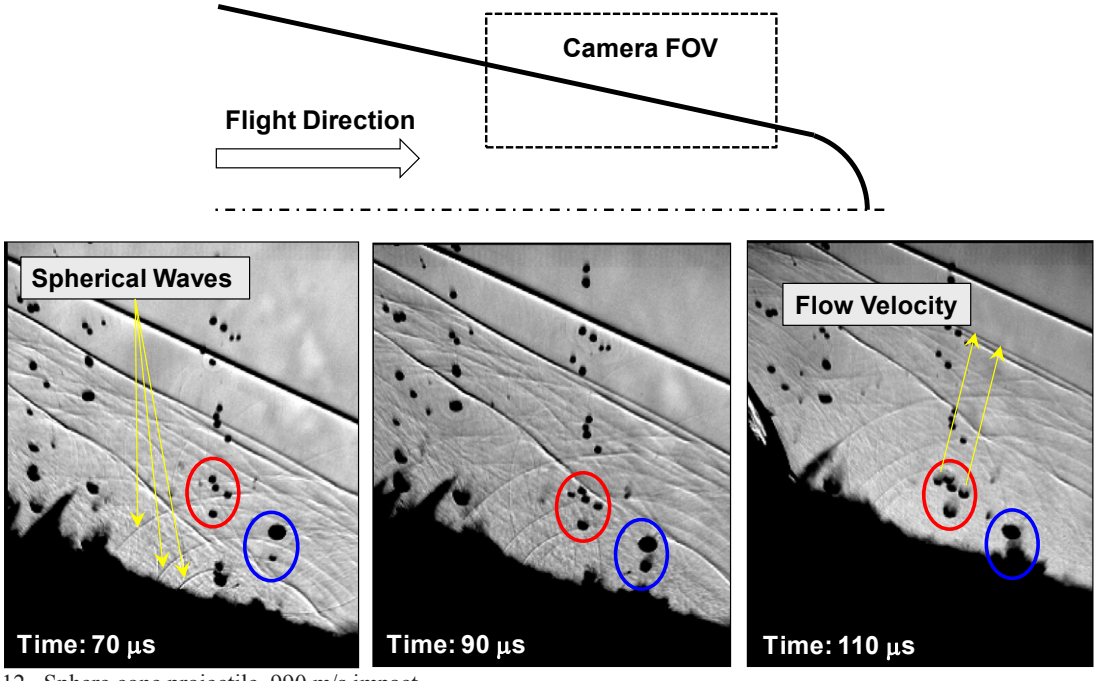

Fig. 12. Sphere cone projectile, 990 m/s impact

projectile surface by extrapolating the orientation of the droplet mass stripping contrail. This relative droplet flow direction has been shown to be nearly perpendicular to the impact surface for a variety of common vehicle shapes to include cones, domes, and ogives [9]. While this result appears counterintuitive, it can be understood by the coordinate transformation from the vehicle frame of reference to that of the droplet. Equation 2 can be used for the transformation where V1 is the vehicle velocity, V_2 is the post-oblique shock velocity calculated from oblique shock relations, and q is the oblique shock flow angle (Figure 13). With this information, the Law of Cosines can be used to determine the inclination angle of the droplet flow. For many cases considered, this angle is typically within 2° of the local surface normal.

$$V_{Drop} = \sqrt{V_1^2 + V_2^2 - 2V_1V_2\cos\theta} \tag{2}$$

The next phase of the test program investigated the shock environment of hemispherical domes. Hemispherical domes are commonly employed as Infrared seeker domes and the typical velocity of such systems are approximately Mach 2. The hemispherical dome utilized was 15.2 cm in diameter which maximized the shock standoff distance for better photographic coverage. Two tests were conducted at similar conditions to capture the demise event. Results of the first test are shown in Fig. 14. The red circles in the figure indicate the initial droplet size and location prior to the shock crossing. The comet-like demise tails are similar to what is commonly captured in shock tube demise studies, and this data indicates that there is sufficient time for droplets to not only change shape, but lose appreciable mass prior to impacting a hemispherical surface at typical flight velocities. This data can also be applied to estimate the effective droplet drag as the temporal droplet position can be extracted from the data. This empirical data combined with the data from Fig. 12 indicate that for a range of vehicle shapes and flight conditions, there is sufficient time for the droplet to not only alter shape, and hence the impact boundary condition, but also lose mass. The opinion that there is insufficient time for droplets to alter their spherical shape prior to impact is not supported by this data and this assumption can no longer be justified. The time required for droplet shape change and mass stripping is a function of the spatial Weber number. While a vehicle that travels at higher velocities will have less distance in the post-shock region for the demise event to occur prior to impact, the post-shock environment Weber number increases with the square of the local droplet velocity and linearly with the post-shock density. These opposing trends work in such a way as to mitigate the effects of the reduced demise time/distance for higher speed vehicles by accelerating the demise event.

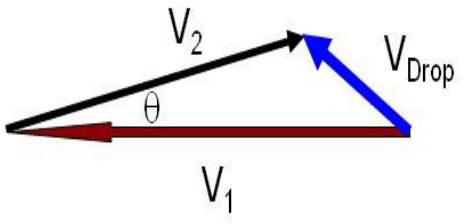

Fig. 13: Droplet coordinate frame

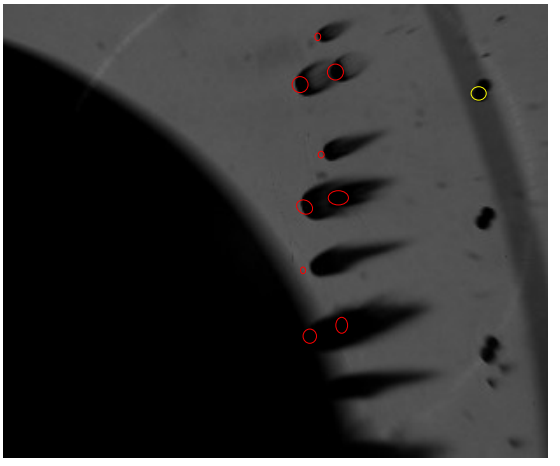

Fig. 14: Hemisphere, 726 m/s impact

The second hemispherical test utilized a shadowgraph technique in order to capture the embedded shock structure of the inner shock region as shown in Fig. 15. Figure 15A shows the entry of a single droplet with two streams of droplets yet to transit the shock. The droplet has both a bow shock and a trailing fan expansion shock. This demonstrates that the post-shock droplet environment is supersonic as indicated from the schematic in Fig. 3. Figure 15B shows the impact of the first droplet and the inclusion of four more droplets into the post-shock flow region. Finally, Fig. 15C shows the complexity of the post-shock droplet environment when multiple droplets exist in the region along with the added complexity associated with the droplet impact events producing ejecta into the region with velocities greater than that of the projectile.

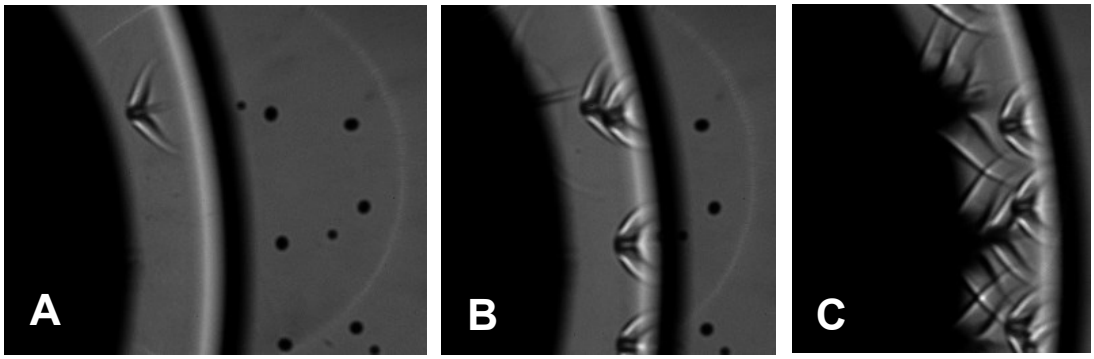

Fig. 15. Hemisphere, 707 m/s impact

6. Conclusion

In order to be assured that a flight system has a sufficiently robust capability to withstand flight through natural adverse environments such as rain, accurate ground test protocols are required. To date, the ground test methods have assumed spherical rain impact events whereby each event can be treated in isolation to all others. This research has demonstrated that for a variety of vehicle induced flowfields, droplets as large as 2-mm in diameter and greater have sufficient time to both alter their initial spherical shape and to also lose mass due to shear induced stripping. It has also demonstrated that while shock tube and tunnel data is useful for numeric code validation studies, it is insufficient to properly characterize the droplet demise event in a vehicle induced flow. State-of-the-art hydrocodes have been employed in order to better understand the associated physics of droplet/flowfield interactions, and have shown promise to help direct future ground test methods. Future efforts will utilize these models to fully couple the droplet flowfield interaction and the impact event to estimate damage thresholds.

As weather encounter is a random event, studies must be performed on a per vehicle basis in order to bound the range of possible impact conditions for a given vehicle system to establish realistic and conservative ground test environments. While more investigation needs to be accomplished on both understanding and modeling the vehicle environment, progress is being made. However, work remains in order to develop material damage models of sufficient accuracy to estimate the true real-world performance of flight vehicles in adverse natural environments.

References

1. Letson, K., Burleson, W., and Ormsby, P., "Aerothermal and Rain Erosion Behavior of Selected Candidate Plastic Radome Materials in Mach 5 Sled Tests," ASME Paper 77-ENAs-16, March 1977.
2. Theofanous,T., Li, G., Dinh, T., and Chang, C.," Aerobreakup in disturbed subsonic and supersonic flow fields," *J. Fluid Mech*., vol. 593, 2007, pp. 131–170.
3. Engel, O., "Fragmentation of Waterdrops in the Zone Behind an Air Shock," *Journal of research of the National Bureau of Standards*, Vol. 60, No. 3, March 1958, pp. 245-280.
4. Hanson, A., Domich, E., and Adams, H., "Shock Tube Investigation of the Breakup of Drops by Air Blasts," *The Physics of Fluids*, Vol. 6, No. 8, Aug 1963, pp. 1070-1080.
5. Wierzba, A. and Takayama, K., "Experimental Investigation of the Aerodynamic Breakup of Liquid Drops," *AIAA Journal*, Vol. 26, No. 11, Nov 1988, pp. 1329-1335.
6. Theofanous, T., Li, G., and Dinh, T.,"Aerobreakup in Rarefied Supersonic Gas Flows," *Trans. Of ASME: J. Fluids Engng*. Vol. 126, July 2004, pp. 516-527.
7. Theofanous,T., Li, G., Dinh, T., and Chang, C.," Aerobreakup in disturbed subsonic and supersonic flow fields," *J. Fluid Mech*., vol. 593, 2007, pp. 131–170.
8. Chen, H., "Two-Dimensional Simulation of Stripping Breakup of a Water Droplet," *AIAA Journal*, Vol. 46, No. 5, May 2008, pp. 1135-1143.
9. Moylan, B.," Raindrop Demise In A High Speed Projectile Flowfield". PhD. dissertation, The University of Alabama in Huntsville, 2010.
10. Moylan, B., Russell, G., (May 2010). Challenges to Electromagnetic Windows Operating in Adverse Natural Environments. 13th Electromagnetic Window Symposium, Pensacola Beach, Florida.
11. Dabora, E., "Production of Monodisperse Sprays," The Review of Scientific Instruments, Vol. 38, No. 4, 1967, pp. 502-506.
12. Stellingwerf, R. F., "Smooth Particle Hydrodynamics," *Advances in the Free-Lagrange Method*, Trease, Fritts, and Crowley, eds., Springer Verlag, 1990, pp. 239.